VOLUME 80 NUMBER 9–10 SEPTEMBER-OCTOBER 2020

Developmental Neurobiology

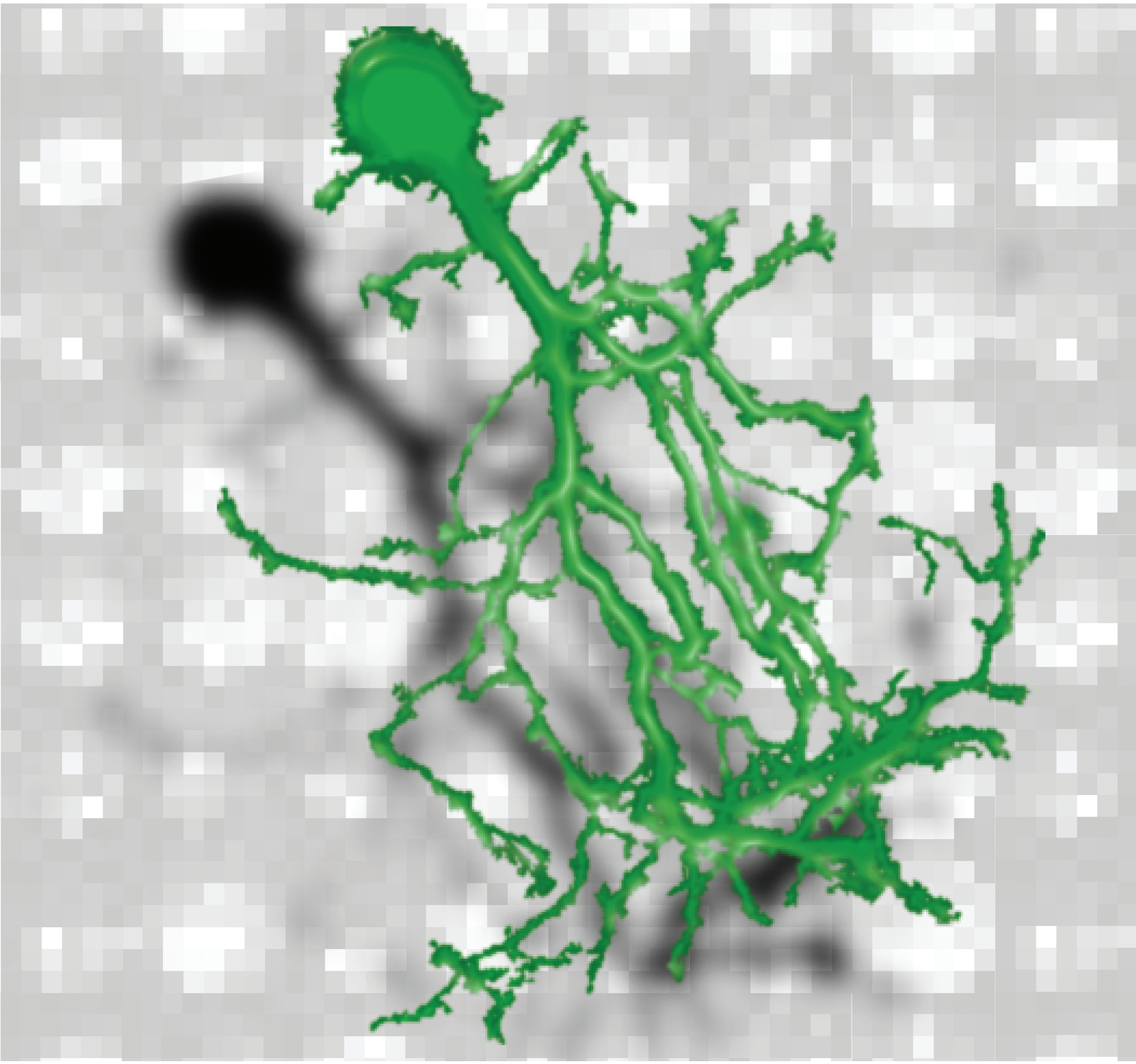

WILEY

Received: 18 February 2020 | Revised: 7 August 2020 | Accepted: 16 September 2020

DOI: 10.1002/dneu.22782

WILEY

RESEARCH ARTICLE

TORC1 selectively regulates synaptic maturation and input convergence in the developing visual system

Delphine Gobert | **Anne Schohl** | **Elena Kutsarova** | **Edward S. Ruthazer**

Montreal Neurological Institute-Hospital, McGill University, Montreal, QC, Canada

Correspondence
Edward S. Ruthazer, Montreal Neurological Institute-Hospital, McGill University, Montreal, Quebec H3A 2B4, Canada.
Email: edward.ruthazer@mcgill.ca

Funding information
Fonds de Recherche du Québec - Santé, Grant/Award Number: postdoctoral fellowship; Canadian Institutes of Health Research, Grant/Award Number: FDN-143238

Abstract

Newly synthesized proteins support the development of functional neural circuits and previous work has suggested that dysregulated translation mediates certain forms of autism spectrum disorder (ASD). Here, we investigated the role of Target of Rapamycin Complex 1 (TORC1) in synaptic and dendritic development in vivo in the retinotectal system of *Xenopus laevis* tadpoles. We found that TORC1 signaling regulates dendritic growth and branching and that acute over-activation of TORC1 by Rheb overexpression drove enhanced maturation of excitatory synapses by recruiting AMPA receptors. Interestingly, TORC1 over-activation did not affect inhibitory transmission, resulting in a significant imbalance in the excitatory-to-inhibitory ratio. Rheb overexpression also enlarged excitatory visual input fields in tectal neurons, consistent with dysregulation of retinotopic input refinement and integration of the cell into the circuit. In contrast to other reports that mainly found impairments in synaptic inhibition using broad systemic deletion or mutation of TORC1 regulatory proteins, our findings from acute, local manipulation of TORC1 reveal its critical role in selectively regulating the number and maturity of excitatory, but not inhibitory, synapses in the developing brain.

KEYWORDS

development, electroporation, mTOR, receptive field, retinotectal, *Xenopus laevis*

1 | INTRODUCTION

During early brain development, neurons in the central nervous system undergo extensive growth and rearrangement of their connections, which ultimately lead to the formation and stabilization of functional synapses. This mechanism has important implications for the proper wiring of the brain. However, how neuronal processes are actually assembled and stabilized into a fully functional circuit is not yet completely understood. At the molecular level, stabilization and maturation of synapses have been associated with changes in the composition of glutamate receptors that are present on the postsynaptic side. More specifically, synaptic maturation involves the addition of α-amino-3-hydroxy-5-methyl-4-isoxazolepropionic acid (AMPA) receptors to "silent" synapses that initially contain only N-methyl-D-aspartate receptor (NMDA) receptors, revealed as an increase in the ratio of AMPA-to-NMDA receptor currents evoked by synaptic stimulation (Haas et al., 2006; Liao et al., 1995; Rajan & Cline, 1998; Wu et al., 1996).

In many systems, short-term plasticity relies on the phosphorylation and trafficking of proteins that are already present at the synapse, while translation and addition of new proteins to the postsynaptic density are critical to sustain long-term synaptic changes. The protein kinase mechanistic target of rapamycin (mTOR) is a master regulator of protein synthesis that can form two distinct complexes: TORC1, when it is associated with the adaptor protein Raptor, and TORC2, when it is associated with

Rictor. The TORC1 complex is sensitive to inhibition by the macrolide rapamycin and can be activated upstream by various kinases converging onto the small GTPase Rheb (Saxton & Sabatini, 2017). Activation of TORC1, but not TORC2, leads to rapid phosphorylation of downstream effectors such as the 4E-BPs and S6K and ultimately to the initiation of translation and ribosome biogenesis (Hay & Sonenberg, 2004; Switon et al., 2017). In the past decade, a number of studies have suggested various roles for mTOR in regulating the dendritic development. Indeed, some groups have reported that interfering with components of the mTOR pathway to decrease the TORC1 activity resulted in smaller and less complex dendritic arbors (Chow et al., 2009; Jaworski et al., 2005; Kumar et al., 2005; Skalecka et al., 2016). Furthermore, there is also in vitro evidence that mTOR can contribute to regulating dendritic spine shape and composition of glutamatergic synapses (Bateup et al., 2011; Henry et al., 2017; Tavazoie et al., 2005).

Neurodevelopmental disorders such as tuberous sclerosis and autism spectrum disorder have been associated with imbalances of protein synthesis and more specifically with dysregulation of components of the mTOR pathway like Tsc1 and 4E-BP2 (Bateup et al., 2011, 2013; Gkogkas et al., 2013; Huang & Manning, 2008). Such dysregulation of protein synthesis leads to a specific increase in the synthesis of neuroligins 1–4 and the AMPA receptor GluA1 and GluA2 subunits (Gkogkas et al., 2013; Ran et al., 2013). These imbalances are thought to favor an increase in the excitation-to-inhibition (E-I) ratio in neural circuits and ultimately have severe consequences on synaptic and behavioral function (Bateup et al., 2011, 2013; Gkogkas et al., 2013; Ran et al., 2013).

In this study, we investigated the consequences of decreasing TORC1-dependent protein synthesis via rapamycin treatment or knockdown of Raptor, and of increasing TORC1-dependent protein synthesis via Rheb overexpression. The use of single-cell electroporation of genetic constructs in vivo has the advantage of tightly restricted temporal and spatial control of expression, reducing the opportunity for homeostatic compensation often observed in mutant animal models. We took advantage of the developing albino *Xenopus laevis* tadpole retinotectal system, which is amenable to both live imaging techniques and in vivo electrophysiology, to gain insight into developmental plasticity mechanisms at both the morphological and functional levels. We found that manipulating TORC1 rapidly affected the dendritic development in vivo and had selective effects on synaptic transmission, only impacting excitatory synapses. The selective increase of AMPA receptor-mediated transmission caused by the activation of TORC1 led to a pronounced imbalance in the E-I ratio and had lasting consequences on the sensory processing of visual information.

2 | MATERIALS AND METHODS

2.1 | Animals

Albino *Xenopus laevis* tadpoles were bred in-house by human chorionic gonadotropin (Sigma)-induced mating as previously described (Munz et al., 2014). Tadpoles were raised on a normal 12 hr light/ 12 hr dark cycle at 21°C in standard Modified Barth's Saline-H (MBSH) unless otherwise specified. All experiments were approved by the MNI Animal Care Committee, in accordance with Canadian Council on Animal Care guidelines.

2.2 | Constructs and reagents

Xenopus laevis Rheb cDNA was obtained from Open Biosystems (GE Healthcare). Lissamine-tagged antisense standard control and *Xenopus laevis* Raptor MOs were obtained from Gene Tools. The sequences were as follows: control MO 5′-CCTCTTACCTCAGTTACAATTTATA-3′, Raptor MO 5′-GGCCGGTGTGTACAGCTCCATTCTT-3′.

pEF-Rheb-myc-2A-EGFP (Rheb + EGFP) construct: a double-stranded oligo was created coding for the following 2A peptide sequence: GSGATNFSLLKQAGDVEENPGP. Restriction sites were added on both sides to facilitate directional cloning. In addition, several restriction sites were inserted at the 5′ end to create a more versatile multiple cloning site. The resulting oligo was inserted into the EcoRI and NotI sites of pEF-EGFP (Addgene plasmid #11154). *Xenopus laevis* Rheb sequence was amplified by PCR, containing part of the 5′UTR and the complete coding sequence (nucleotide sequence nt −100 to nt 554, accession number NM_001087025) and inserted into the ClaI and SpeI sites of pEF-2A-EGFP, resulting in pEF-Rheb-2A-EGFP. Finally, a double-stranded oligo, coding for the myc-sequence (EQKLISEEDL), was inserted into the SpeI and NheI sites of pEF-Rheb-2A-EGFP.

D-AP5 and picrotoxin (PTX) were obtained from Tocris Bioscience and tetrodotoxin (TTX) was obtained from Alomone labs. All other drugs were from Sigma-Aldrich.

2.3 | Electroporation

Tectal neurons were bulk electroporated as previously described (Ruthazer et al., 2005). Briefly, stage 42–43 tadpoles were anesthetized in MBSH supplemented with 0.02%

MS-222 (Sigma) before being transferred to the electroporation stage. Plasmid DNA (1–3 μg/ μl in ddH20) colored with Fast Green was pressure injected into the ventricle using a glass micropipette. Two platinum electrodes were then positioned on each side of the brain and current pulses with the following parameters were delivered using a Grass SD9 stimulator (Grass Instruments): 36 V, 1.6 ms, 3 pulses for each polarity. A 3 μF capacitor was connected in parallel to generate an exponential decay current pulse. Positive fluorescently labeled neurons were used for subsequent electrophysiology experiments 48–72 hr after transfection.

For single-cell labeling, individual tectal neurons were transfected by single-cell electroporation, for which a borosilicate glass micropipette (Sutter Instruments) containing plasmid DNA (1 μg/μl) was gently introduced into the brain of anesthetized stage 44–45 tadpoles to deliver brief trains of current pulses with the following parameters: 30–50 V, two 200 Hz trains of 0.5 s duration each. For some experiments, lissamine-tagged MO (1 μg/μl) was mixed with the plasmid DNA and the polarity of the pulses was alternated. Labeled neurons were first imaged on the day following single-cell electroporation.

2.4 | Electrophysiology

Stage 46–47 tadpoles were anesthetized in MBSH supplemented with 0.02% MS-222 and the brain and overlying skin were filleted along the midline to expose the ventricular surface in an external solution that contained (in mM): 115 NaCl, 4 KCl, 5 HEPES, 10 glucose, 3 $CaCl_2$ and 3 $MgCl_2$, pH 7.3, 250 mOsm. Brains were then laid flat on a Sylgard insert in a submerged recording chamber and maintained at room temperature. Cells were visualized with an Olympus 60× 0.8NA water-immersion objective mounted on an Olympus BX61W upright microscope with a CCD camera (Thorlabs). Miniature excitatory and inhibitory postsynaptic currents (mEPSCs and mIPSCs) were recorded from fluorescent tectal neurons using 8–12 MΩ borosilicate patch pipettes (Sutter Instruments) filled with an internal solution that contained (in mM): 90 $CsMeSO_4$, 5 $MgCl_2$, 20 TEA-Cl, 10 EGTA, 20 HEPES, 2 ATP, 0.3 GTP, and pH 7.3, 250 mOsm. For some experiments external solution was supplemented with 1 μM TTX and 100 μM PTX or 50 μM D-AP5. Cells were voltage-clamped at −60 mV and 0 mV to record mEPSCs and mIPSCs, respectively. Series resistance (20–60 MΩ), input resistance (>1 GΩ), and holding current (< 20 pA) were monitored throughout the experiment and if parameters changed by more than 20%, cells were excluded from analysis.

To record evoked postsynaptic currents, a tungsten bipolar stimulating electrode (FHC) was carefully positioned on the optic chiasm to deliver 0.1 ms constant current pulses every 20 s using a stimulus isolation unit (WPI). Evoked postsynaptic currents were recorded using 8–12 MΩ borosilicate patch pipettes (Sutter Instruments) filled with an internal solution that contained (in mM): 100 K-gluconate, 8 KCl, 5 NaCl, 1.5 MgCl2, 20 HEPES, 10 EGTA, 2 ATP, 0.3 GTP, pH 7.3, Osm 250, and supplemented with 100 μM PTX. Cells were voltage-clamped at −60 mV or +55 mV to record AMPA and NMDA currents, respectively.

Recordings were obtained using a MultiClamp 700B amplifier (Molecular Devices). Signals were digitized at 10 kHz and filtered at 2 kHz (Digidata 1440A; Molecular Devices) for offline analysis using MiniAnalysis (Synaptosoft) or Axograph X (John Clements).

2.5 | Receptive field mapping

Selected stage 46–47 tadpoles were first immobilized by intraperitoneal injection of D-tubocurarine (2.5 mM). Tadpoles were then transferred to the recording chamber and held in place in a custom-shaped Sylgard submerged chamber using insect pins. The brain and overlying skin were then filleted along the midline and a broken patch pipette was used to carefully expose fluorescently labeled tectal neurons. To ensure that all EGFP-positive cells also expressed Rheb protein, we transfected a single Rheb-2A-EGFP plasmid, from which both proteins are translated sequentially from a single message. Expression of this construct gave increases in mEPSC amplitude and frequency, compared to an EGFP control plasmid, that were similar to those seen using co-electroporation of independent EGFP and Rheb constructs (data not shown). A multicore optical image fiber (FIGH-30 – 650S, Myriad Fiber) coupled to a projector (Optoma) was placed in front of the contralateral eye for presenting visual stimuli generated using custom ImageJ macros. White squares on a black background arranged on a 7 × 7 grid were presented in a random fashion for 1 s every 5 s, until the entire receptive field was mapped. All stimuli were presented twice to reduce possible contamination by spontaneous activity.

Light-evoked compound synaptic currents (CSCs) were recorded using 8–12 MΩ borosilicate patch pipettes (Sutter Instruments) filled with an internal solution that contained (in mM): 100 K-gluconate, 8 KCl, 5 NaCl, 1.5 $MgCl_2$, 20 HEPES, 10 EGTA, 2 ATP, 0.3 GTP, pH 7.3, and 250 mOsm. Cells were voltage-clamped at −60 mV and 0 mV to record excitatory and inhibitory CSCs, respectively. Only neurons for which both the light-evoked eCSCs and iCSCs were successfully recorded were included in the analysis.

2.6 | Two-photon imaging

Daily images of single tectal neurons were acquired on a custom-built Olympus FV300 microscope equipped with an Olympus LUMPFL 60x water immersion objective (1.1 NA). Excitation light was provided by a MaiTai-BB Ti:Sapphire

femtosecond pulsed IR laser (Spectra Physics). Optical z-series were collected at 1 μm intervals using Fluoview software. All image z-stacks were denoised using the CANDLE software implemented in MATLAB (Coupé et al., 2012). 3D reconstruction of single neurons was performed using Imaris (Bitplane).

2.7 | Western blotting

Samples for Western blotting experiments were obtained as follows:

Samples were extracted in 10 mM HEPES pH 7.4, 120 mM NaCl, 1% NP40, and supplemented with phosphatase inhibitors (Halt Protease and Phosphatase, Thermo Scientific). Samples were then separated by SDS-PAGE on a 10% acrylamide gel and transferred onto a PVDF membrane. Depending on the experiment the membrane was stained with the following antibodies: rabbit anti-phospho-p70S6K (Cell Signaling, 9205S, RRID: AB_330944), rabbit anti-p70S6K (Cell Signaling, 9202S, RRID: AB_331676), rabbit anti-GluA1 (Abcam ab109450, RRID:AB_10860361), rabbit anti-GluA2 (Abcam ab133477; RRID: AB_2620181) 1:5,000 dilution each, rabbit anti-βtubulin (Santa Cruz, sc-9104, RRID:AB_2241191) 1:20,000, rabbit anti-histone H3 (Cell Signaling 9,715, RRID:AB_331563) 1:50,000, secondary antibodies: Goat anti-Rabbit HRP (Jackson Immunoresearch, 111-035-144, RRID: AB_2307391). Blots were developed using Immobilon Western Chemiluminescent HRP substrate, Millipore Sigma, WBKLS0100.

Rapamycin experiment:

Animals were raised in 0.1× MBSH supplemented with 10 μM rapamycin from stage 30 to stage 47. Animals were then anesthetized in MBSH with 0.02% MS-222 and brains were dissected and processed for sample extraction.

Raptor MO experiment:

Embryos were injected in each blastomere at the two-cell stage with 18–40 ng of either lissamine-tagged control MO or Raptor MO. Protein was then extracted from lissamine-positive animals at stage 33/34.

Rheb overexpression:

Stage 43 tadpole brains were bulk electroporated with two plasmids encoding *Xenopus* Rheb and EGFP at a concentration of 2 μg/μl and 1 μg/μl, respectively. At stage 47, brains of EGFP positive animals were dissected.

2.8 | Experimental design and statistical analyses

Data are presented as mean ± *SEM*. Statistical analysis was performed using GraphPad Prism 6.0 (GraphPad Software). Data were tested for normality using a K-S test and Welch's correction for heteroscedasticity was used where required. Two-tailed tests were used for all analyses except that one-tailed, one-sample tests were used to verify that glutamate receptor expression was decreased in rapamycin-treated animals. The statistical tests used are described in the figure legends.

For miniature postsynaptic current recordings, 100 randomly selected events were analyzed per cell. Threshold amplitude was set at 4 pA. To measure AMPA/NMDA ratios, we used the peak amplitude at −60 mV to calculate the AMPAR component and the amplitude between 15 and 25 ms after the onset of the response at +55 mV to calculate the NMDAR component. For receptive field mapping experiments, we measured the total synaptic charge transfer for 500 ms after the onset of each visual stimulus. All CSCs were normalized to the maximum response for that cell to generate gray scale receptive field maps. For measuring receptive field size, all responses that were at least three times the standard deviation of spontaneous activity were counted as a visually responsive location.

3 | RESULTS

3.1 | Specific TORC1 inhibition impairs dendritic arbor formation

To investigate the consequences of blocking TORC1-dependent protein synthesis on dendritic morphogenesis, we first assessed whether raising tadpoles in rapamycin, a specific mTOR inhibitor, could reduce the phosphorylation of S6K, one of TORC1's main downstream effectors (Figure 1a). Western blot analysis demonstrated that exposing tadpoles to rapamycin (10 μM) for 48 h reduced the phosphorylation of S6K in the brain (Figure 1b), confirming that in our system, rapamycin treatment decreases TORC1 activity (p-S6K/ total S6K: 53 ± 6.1% compared to paired controls, $n = 3$ experiments). We then evaluated whether blocking TORC1 signaling could impact dendritic arborization of tectal neurons in vivo. We monitored the morphology of individual tectal neurons that had been electroporated to express EGFP over four consecutive days. Individual cells were imaged daily in vivo by two-photon laser-scanning microscopy (Figure 1c,d) and after the first imaging session (day 1), tadpoles were either returned to a normal rearing solution or raised in a solution supplemented with rapamycin (10 μM). In tadpoles that were raised in rapamycin, dendritic growth was dramatically decelerated, resulting in significantly smaller dendritic arbors (Figure 1e, day 4:1643.80 ± 244.66 μm, $n = 7$ for control cells versus 1,085.57 ± 84.26 μm, $n = 7$ for rapamycin-treated cells) with fewer dendritic branch tips

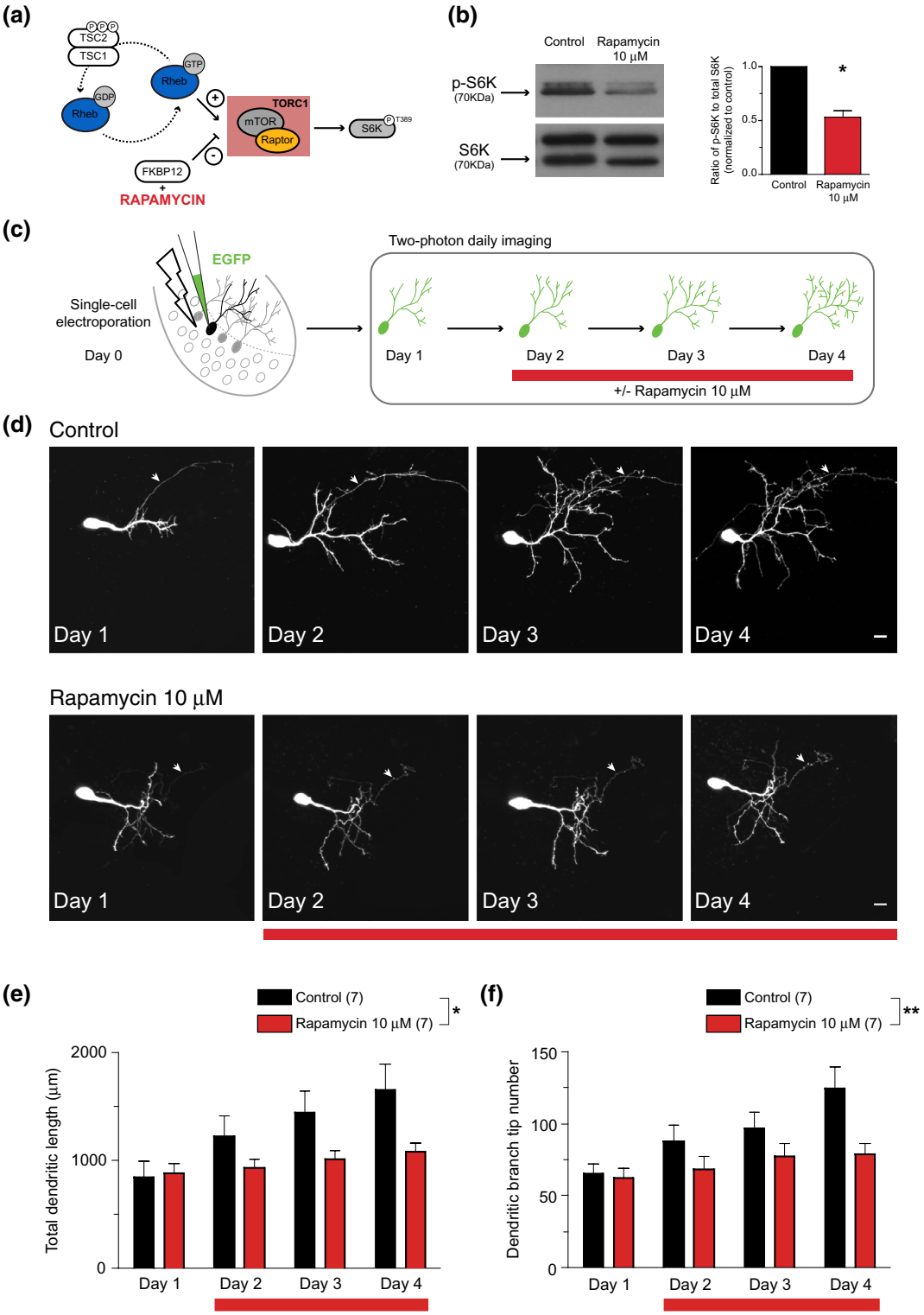

FIGURE 1 Rapamycin treatment impairs dendritic arbor growth and decreases dendritic complexity of tectal neurons. (a) Schematic representation of the TORC1 pathway. (b) Western blot showing rapamycin-treated stage 47 tadpole brains (10 μm for 48 h) have lower levels of S6K phosphorylation compared to paired controls (one-sample *t*-test, $p = .0165$, $n = 3$ experiments). (c) Schematic representation of the experimental imaging protocol. (d) Representative images of EGFP-expressing neurons from both control- and rapamycin-treated tadpoles imaged over four consecutive days (scale bar = 10 μm). White arrows indicate axonal projection. (e-f) Summary bar graphs show that TORC1 inhibition results in smaller total arbor size (main effect by two-way ANOVA $*p = .0104$) (e) and reduced branch tip number (main effect by two-way ANOVA $**p = .0058$) (f), suggesting that TORC1 inhibition can significantly stunt dendritic arbor formation and decrease dendritic complexity [Color figure can be viewed at wileyonlinelibrary.com]

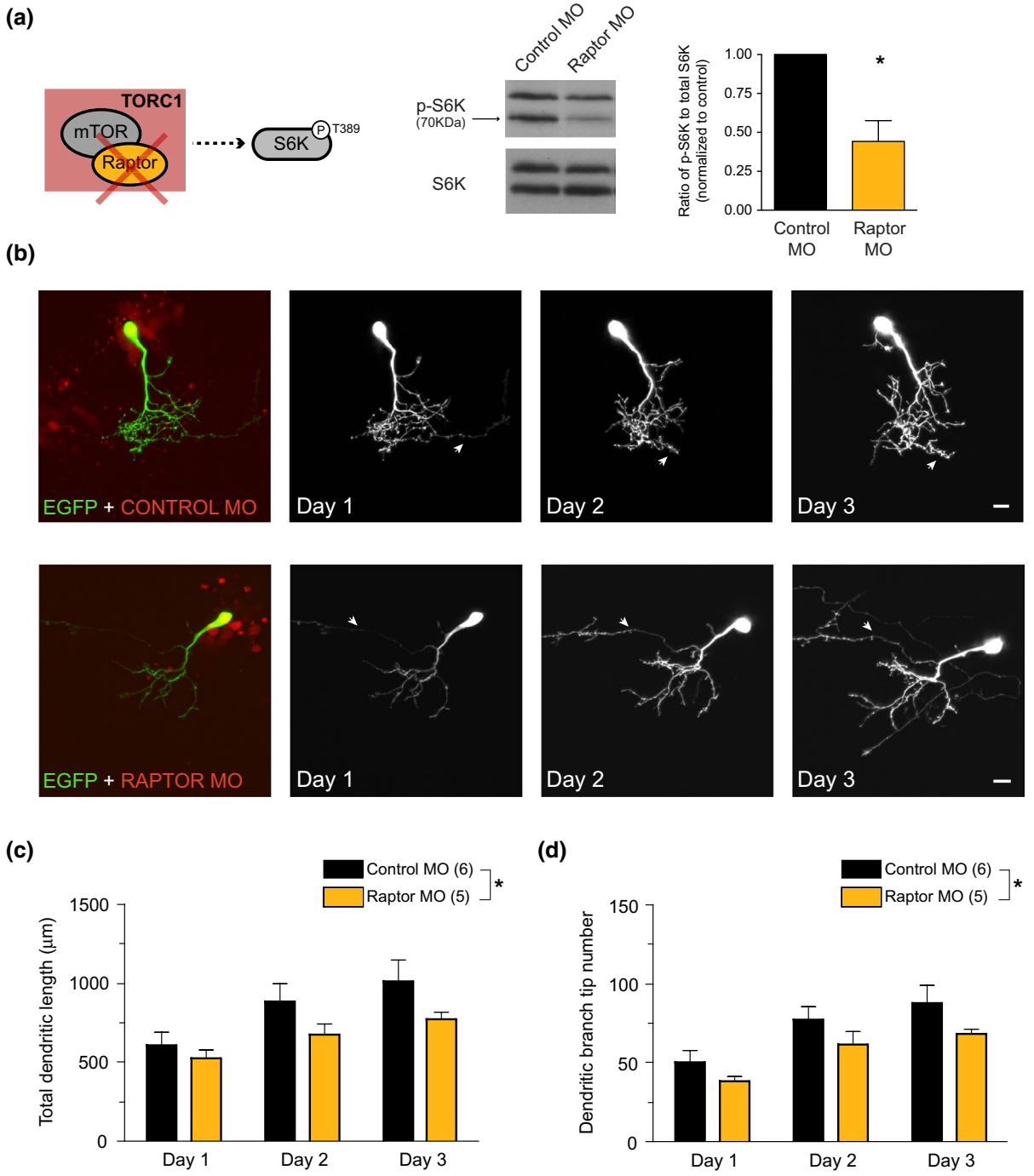

FIGURE 2 Single-cell knockdown of Raptor impairs dendritic arbor formation and decreases dendritic complexity of tectal neurons. (a) Western blot showing that animals injected at the two-cell stage with Raptor MO and extracted at stage 33–34 present lower levels of phosphorylated S6K than animals injected with control MO (one-sample *t*-test, $p = .0245$, $n = 4$ experiments) (b) Representative images of neurons co-electroporated with EGFP plasmid (green) and either lissamine-tagged (red) antisense control MO or Raptor MO imaged over three consecutive days (scale bar = 10 µm). White arrows indicate axonal projection. (c-d) Summary bar graphs show that specific TORC1 inhibition by Raptor MO electroporation significantly reduces both total arbor size (main effect by two-way ANOVA $*p = .0412$) (c) and branch tip number (main effect by two-way ANOVA $*p = .0375$) (d) demonstrating that specific TORC1 inhibition can significantly stunt dendritic arbor formation and decrease dendritic complexity. $*p < .05$

than cells in control tadpoles (Figure 1f, day 4:125 ± 16 branches, $n = 7$ for control cells versus. 79 ± 8 branches, $n = 7$ for rapamycin-treated cells).

It has previously been reported in the literature that prolonged exposure to high doses of rapamycin not only interferes with TORC1 function but could also affect TORC2

(Sarbassov et al., 2006). Therefore, to confirm that the observed effects were principally mediated by TORC1 inhibition, we created a red fluorescent lissamine-tagged antisense morpholino oligonucleotide (MO) against the TORC1 component protein Raptor. Western blot analysis revealed that tadpoles injected at the two-cell stage with Raptor MO had significantly reduced levels of phosphorylated S6K compared to tadpoles injected with standard control MO (Figure 2a, p-S6K/ total S6K: 44 ± 13% compared to paired controls, $n = 4$ experiments). We then co-electroporated single tectal neurons to express EGFP along with either control MO or Raptor MO and followed their morphology for three consecutive days (Figure 2b). Similarly to neurons treated with rapamycin, Raptor knockdown neurons had significantly smaller dendritic arbors (Figure 2c, on day 3:1,012.48 ± 143.79 μm, $n = 6$ for control MO versus 771.73 ± 52.56 μm, $n = 5$ for Raptor MO) and significantly fewer dendritic branch tips (Figure 2d) than cells with control MO (on day 3:88 ± 12

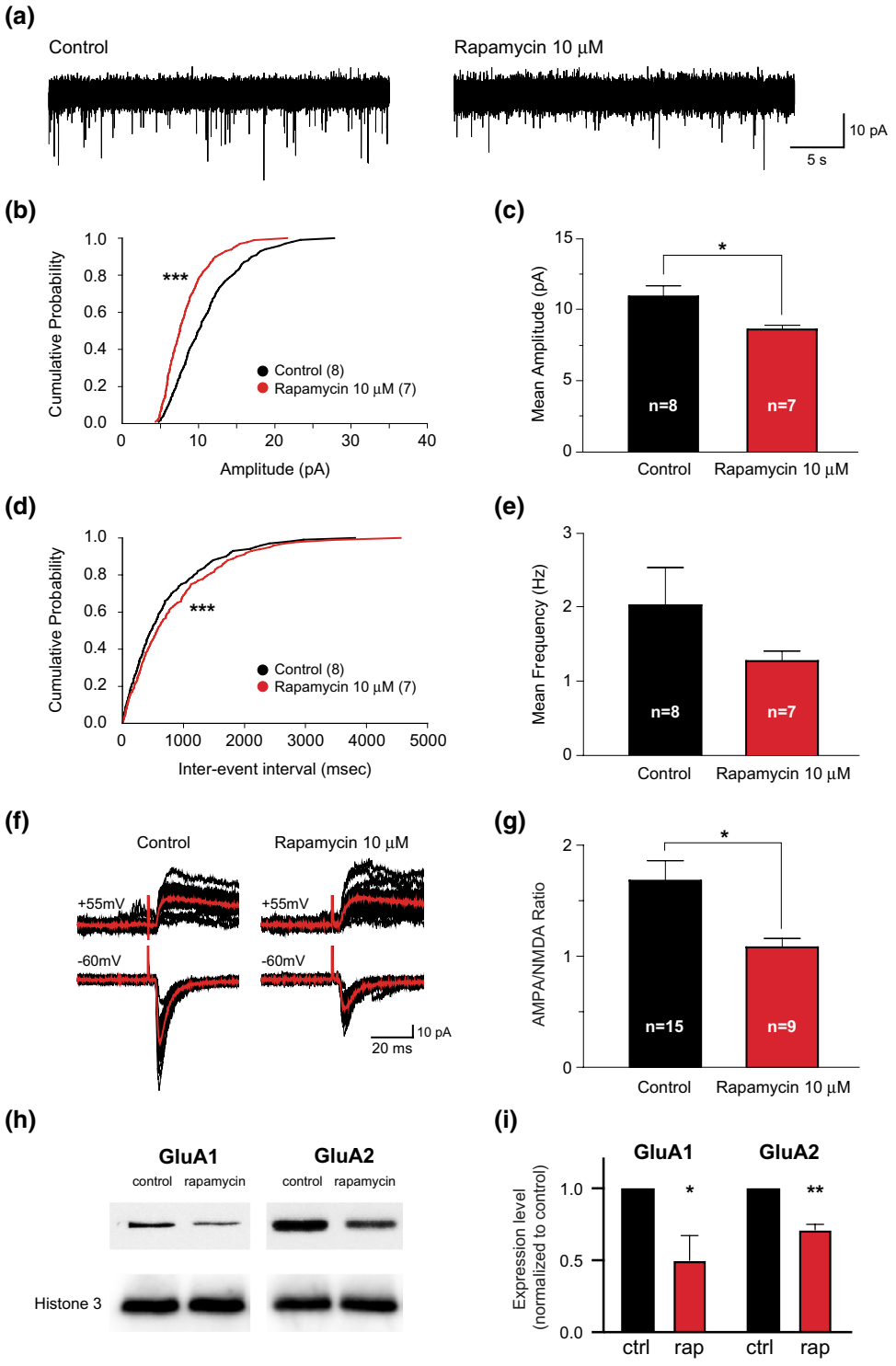

FIGURE 3 Rapamycin treatment impairs synaptic maturation of tectal neurons. (a) Representative whole-cell traces of AMPA mEPSC recordings from control- and rapamycin-treated tadpoles (10 μM for 48 h). Miniature postsynaptic currents were recorded at −60 mV. Cumulative probability plot (b) and summary bar graph (c) of AMPA mEPSC amplitude (100 events per cell) show that TORC1 inhibition by rapamycin significantly reduces AMPA mEPSC amplitudes (K-S test, ***$p < .001$; two-tailed t-test with Welch's correction, *$p = .0167$), suggesting that TORC1-dependent protein synthesis is necessary for normal developmental synaptic maturation. D,E Cumulative probability plot (d) showing rapamycin treatment increases AMPA mEPSC inter-event intervals (K-S test, ***$p < .001$) and summary bar graph of AMPA mEPSC frequency (e) (two-tailed t-test with Welch's correction $p = .2734$). (f) Representative whole-cell traces (red: average of 20 consecutive evoked EPSCs) of evoked NMDAR and AMPAR-mediated EPSCs (recorded at +55 mV and −60 mV, respectively), from both control- and rapamycin-treated tadpoles. (g) Summary bar graph shows that rapamycin treatment significantly reduces AMPA/NMDA ratios, suggesting that TORC1 activity normally promotes the maturation of retinotectal synapses (Mann-Whitney test, *$p < .0297$). (h) Western blots of GluA1 and GluA2 for control- and rapamycin-treated animals. Histone 3 was used in place of tubulin as a loading control to avoid artifacts from differential dendritogenesis. (i) Quantification of GluA1 and GluA2 expression from paired control- and rapamycin-treated brains. (one-sample t-tests, GluA1: *$p = .05$, GluA2: **$p = .0083$, $n = 3$ experiments) [Color figure can be viewed at wileyonlinelibrary.com]

branches, $n = 6$ for control MO versus. 68 ± 4 branches, $n = 5$ for Raptor MO).

Taken together, these results demonstrate that inhibiting TORC1 in tectal neurons, either by rapamycin treatment or knockdown of Raptor, impairs dendritic arbor formation and significantly reduces dendritic complexity.

3.2 | Specific TORC1 inhibition impairs synapse maturation

During the development of the visual system, nascent "silent" glutamatergic synapses undergo maturation by the incorporation of AMPA receptors at NMDAR-only synapses (Wu et al., 1996). We next evaluated whether interfering with TORC1 signaling by rapamycin treatment could impact synaptic development, by recording whole-cell AMPAR-mediated miniature excitatory postsynaptic currents (mEPSCs) in tectal neurons. AMPA mEPSCs were measured by voltage clamping tectal cells at −60 mV in 1μm TTX (Figure 3a). We found that raising tadpoles in rapamycin for 48 hr resulted in significantly smaller mEPSC amplitudes compared to control tadpoles (Figure 3b,c, 10.95 ± 0.82 pA, $n = 8$ for control cells vs. 8.36 ± 0.35 pA, $n = 7$ for rapamycin-treated cells) suggesting that TORC1 inhibition prevents normal developmental synapse maturation. Moreover, rapamycin-treated tadpoles had increased inter-event intervals (Figure 3d) and appeared to have slightly decreased mEPSC frequencies (Figure 3e, 2.00 ± 0.54 Hz, $n = 8$ for control cells vs. 1.34 ± 0.15 Hz, $n = 7$ for rapamycin-treated cells), consistent with TORC1 inhibition affecting the number of mature synapses. To assess if the changes in mEPSC frequency, which typically reflect alterations in the number of mature synapses on the postsynaptic side, might instead reflect presynaptic changes, we also measured paired-pulse ratios. We observed no difference in paired-pulse facilitation at all three inter-event intervals tested between control-and rapamycin-treated tadpoles (Supporting Figure S1), indicating that changes in presynaptic release probability are unlikely to account for the observed effects on mEPSC frequency.

In addition to the quantification of mEPSC properties, we also evaluated the effect of rapamycin on AMPA/NMDA ratios evoked by optic nerve stimulation at the chiasm to specifically measure retinotectal synapse maturation (Figure 3f,g). We observed that tadpoles raised in rapamycin presented significantly smaller AMPA/NMDA ratios than the control tadpoles (1.69 ± 0.19, $n = 15$ for control cells vs. 1.08 ± 0.09, $n = 9$ for rapamycin-treated cells), indicating that retinotectal synapses in rapamycin-treated tadpoles have fewer AMPA receptors and are, therefore, less mature, in agreement with the observed reduction of mEPSC amplitude in the same group of animals. Further support for this conclusion came from western blot analysis showing significantly reduced levels of GluA1 and GluA2 subunits of the AMPA receptor in brain homogenates from rapamycin-reared animals normalized to paired controls (Figure 3h,i, GluA1: 50.0 ± 12.5%, GluA2: 71.2 ± 12.5%, $n = 3$ experiments).

In agreement with our observations in rapamycin-treated tadpoles, mEPSC amplitudes in tectal neurons co-electroporated with EGFP and Raptor MO were also significantly smaller than those of either control untreated EGFP neurons or EGFP neurons with control MO (Figure 4a-c) (11.31 ± 1.01 pA, $n = 9$ for untransfected cells and 11.82 ± 1.18 pA, $n = 7$ for control MO versus. 8.00 ± 0.53 pA, $n = 7$ for Raptor MO), lending further support to the idea that TORC1 inhibition impairs synapse maturation. Moreover, Raptor MO expression significantly increased inter-event intervals (Figure 4d) and decreased mEPSC frequency (Figure 4e, 1.21 ± 0.10 Hz, $n = 9$ for untransfected cells and 1.21 ± 0.21 Hz, $n = 7$ for control MO versus. 0.66 ± 0.10 Hz, $n = 7$ for Raptor MO), indicating that specific suppression of TORC1 function results in fewer mature functional synapses.

Taken together, these data show that TORC1 inhibition by either rapamycin treatment or knockdown of Raptor has profound effects on AMPAR-mediated synaptic transmission

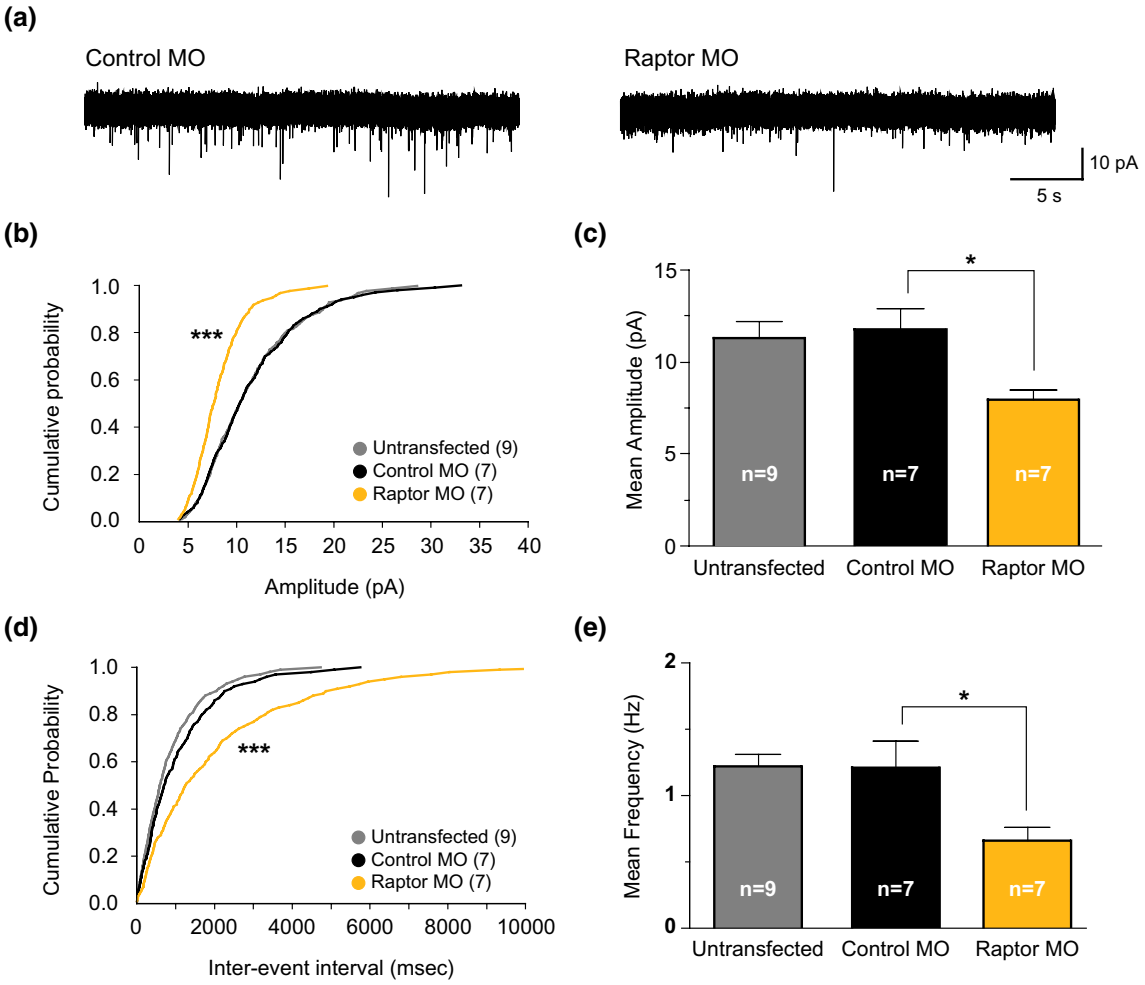

FIGURE 4 Knockdown of Raptor impairs synaptic maturation of tectal neurons. (a) Representative whole-cell traces of AMPA mEPSC recordings from control MO and Raptor MO-positive cells. Cells were held at −60 mV. (b,c) Cumulative probability plot (b) and summary bar graph (c) of AMPA mEPSC amplitudes (100 events per cell) show that specific TORC1 inhibition by introducing Raptor MO significantly reduces AMPA mEPSC amplitudes (K-S test, ***$p < .001$; one-way ANOVA $p = .0285$ with Bonferroni's multiple comparisons test *$p < .05$), suggesting that TORC1-dependent protein synthesis is necessary for normal developmental synaptic maturation. (d,e) Cumulative probability plot of AMPA mEPSC inter-event intervals (d) and summary bar graph of AMPA mEPSC frequency (e) show that TORC1 inhibition also significantly increases AMPA mEPSC inter-event intervals (K-S test, ***$p < .001$) and decreases mEPSC frequencies (one-way ANOVA $p = .0168$ with Bonferroni's multiple comparisons test *$p < .05$), suggesting that specific TORC1 inhibition results in fewer functional synapses [Color figure can be viewed at wileyonlinelibrary.com]

and can significantly impair retinotectal synapse maturation and decrease functional synapse number.

3.3 | TORC1 activation increases dendritic arbor size and complexity

Decreasing TORC1 activity had important effects on both dendritic morphology and synapse maturation. However, it is unclear whether the observed effects were due to a general decrease of protein synthesis leading to scarce cellular resources or reflected a specific regulation of proteins necessary to build and stabilize nascent synapses. To begin addressing this question, we performed a series of experiments in which TORC1 activity was upregulated by overexpression of Rheb, a selective upstream activator of TORC1 (Figure 1a).

We first tested whether overexpressing Rheb would result in increased S6K phosphorylation, indicative of TORC1 activation. To this end, we performed Western blot analysis and demonstrated that expression of a plasmid encoding *Xenopus laevis* Rheb in tectal neurons increased the phosphorylation of S6K in the brain (Figure 5a, 57.0 ± 7.5% increase, $n = 3$ experiments). We next electroporated single tectal neurons to express either EGFP or EGFP plus Rheb and followed their morphology over three consecutive days (Figure 5b). Neurons overexpressing Rheb presented significantly bigger dendritic arbors (Figure 5c, on day 3:1,080.91 ± 130.50 μm, $n = 8$ for EGFP cells vs. 2,174.56 ± 295.78 μm, $n = 7$ for Rheb + EGFP cells) and

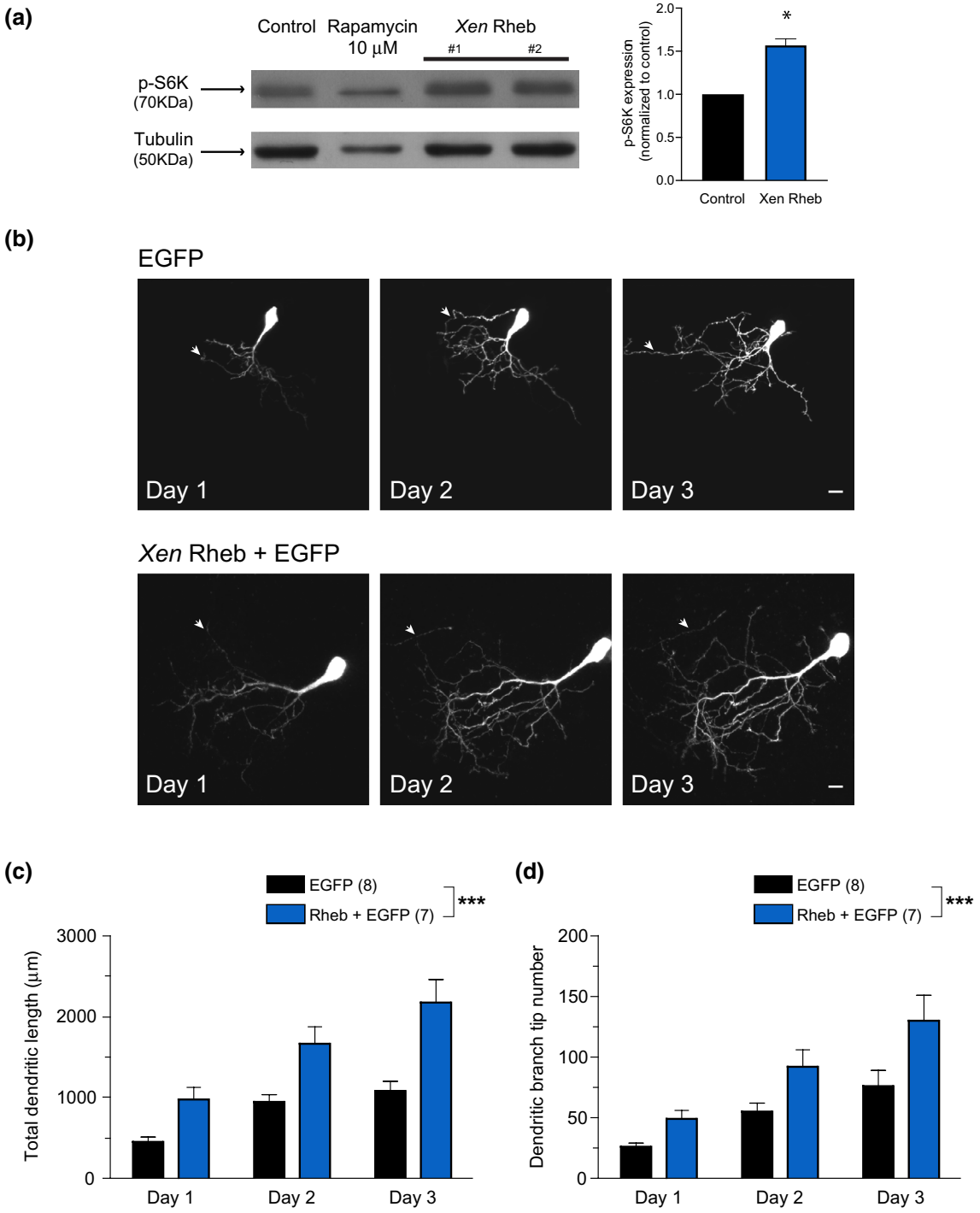

FIGURE 5 Rheb activation promotes dendritic arbor formation and increases dendritic complexity of tectal neurons. (a) Western blot showing that tadpole brains overexpressing *Xenopus laevis* Rheb, in contrast to rapamycin-treated animals, present higher levels of phosphorylated S6K than control brains (one-sample *t*-test, $*p = .0168$, $n = 3$ experiments). (b) Representative images of EGFP or *Xenopus laevis* Rheb + EGFP-expressing neurons imaged over three consecutive days (scale bar = 10 μm). White arrows indicate axonal projection. (c,d) Summary bar graphs show that TORC1 activation significantly increases both total arbor size (main effect by two-way ANOVA, $***p < .0001$) (c) and branch tip number (main effect by two-way ANOVA, $***p = .0010$) (d), suggesting that TORC1 activation is sufficient to promote dendritic arbor formation and increase dendritic complexity [Color figure can be viewed at wileyonlinelibrary.com]

had more dendritic branch tips (Figure 5d) than the control neurons (on day 3:76 ± 14 branches, $n = 8$ for EGFP cells vs. 130 ± 22 branches, $n = 7$ for Rheb + EGFP cells). These results suggest that TORC1 activation by Rheb overexpression can promote the dendritic arbor growth and increase the dendritic complexity.

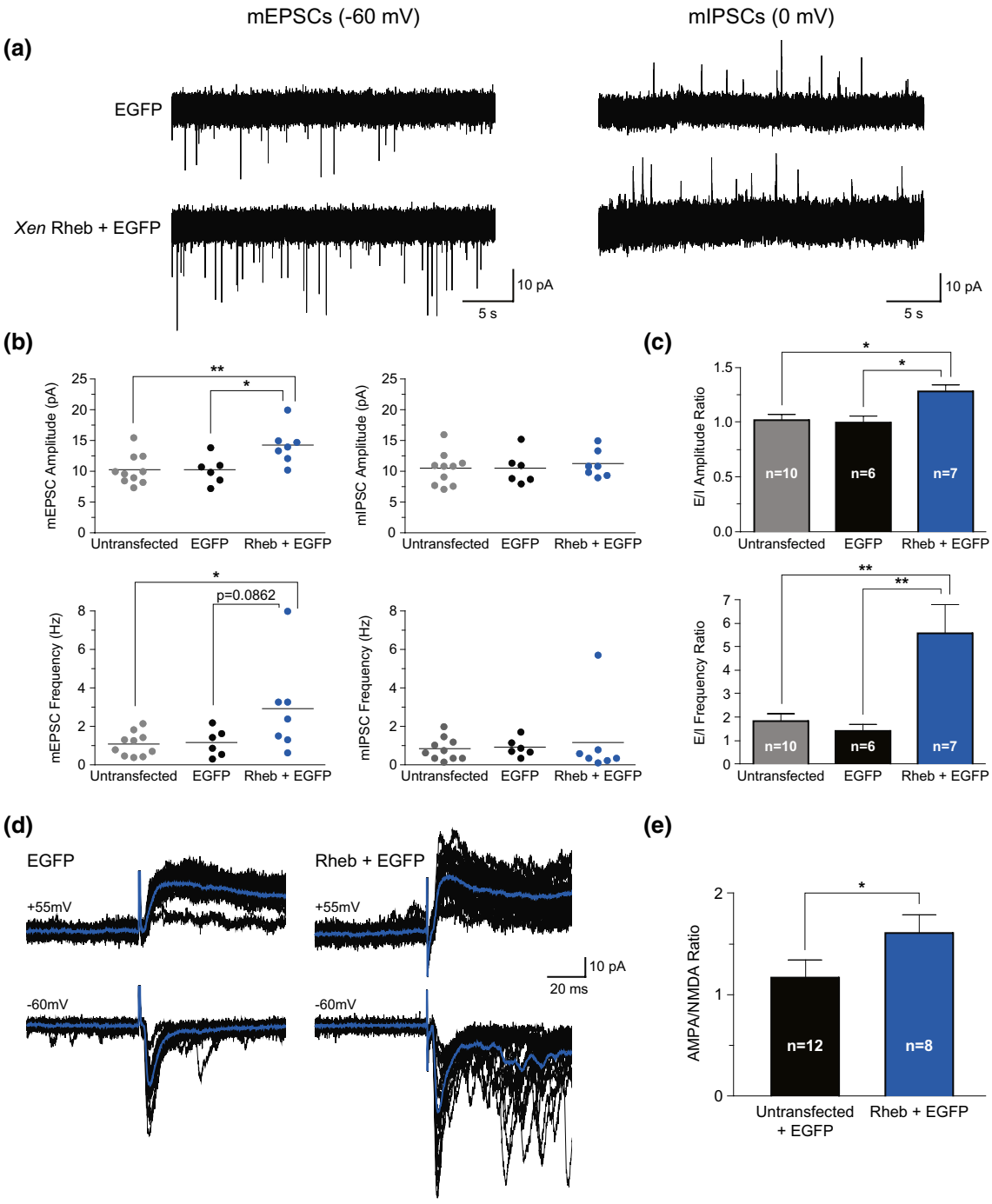

FIGURE 6 Rheb activation leads to an imbalance in excitation-to-inhibition ratio by specifically promoting excitatory synaptic maturation of tectal neurons. (a) Representative whole-cell traces of AMPAR-mediated mEPSC (left) and GABA receptor-mediated mIPSC recordings (right) from both EGFP only and *Xenopus laevis* Rheb + EGFP expressing cells. (b) Summary bar graphs show that Rheb overexpression specifically increases mEPSC amplitude and frequency (*upper left*: one-way ANOVA $p = .0126$ with Bonferroni's multiple comparison test $^*p < .05$; *lower left*: one-way ANOVA $p = .0418$ with Bonferroni's multiple comparison test $^*p < .05$), with no effect on mIPSCs (*upper right*: one-way ANOVA $p = .8266$; *lower right*: one-way ANOVA $p = .8542$), which significantly shifts the E/I ratio (c) (amplitude: one-way ANOVA $p = .0125$ with Bonferroni's multiple comparison test $^*p < .05$; frequency: one-way ANOVA $p = .0015$ with Bonferroni's multiple comparison test $^{**}p < .01$) and suggests that TORC1 activation specifically upregulates the excitatory transmission. (d) Representative whole-cell traces (blue: average of 20 consecutive evoked EPSCs) of evoked NMDAR and AMPAR EPSCs (recorded at +55 mV and −60 mV, respectively), comparing untransfected and EGFP-expressing cells with *Xenopus laevis* Rheb + EGFP cells. (e) Summary bar graph shows that Rheb overexpression significantly increases AMPA/NMDA ratios, consistent with the idea that TORC1 activation can promote the maturation of retinotectal synapses (Mann-Whitney test, $^*p < .05$) [Color figure can be viewed at wileyonlinelibrary.com]

3.4 | TORC1 activation selectively upregulates excitatory transmission leading to an imbalance in the E-I ratio

We next investigated whether increasing TORC1 activity by overexpressing Rheb could also affect synapse maturation and whether this might differentially impact excitatory and inhibitory synapses. Previous work on mouse models of tuberous sclerosis (Bateup et al., 2011, 2013) or ASDs (Gkogkas et al., 2013) reported that dysregulated mTOR signaling can lead to an imbalance in the E-I ratio. However, it is not clear whether this results primarily from an increase in excitatory function or a reduction of inhibition, as the E-I ratio is subject to homeostatic compensation over time in transgenic models (Antoine et al., 2019). In contrast, the extremely precise spatiotemporal control of gene expression afforded by our in vivo single-cell electroporation approach can reveal effects that, at least initially, are less impacted by compensation.

We, therefore, measured both AMPA-mediated mEPSCs and GABA-mediated miniature inhibitory postsynaptic currents (mIPSCs) in the same tectal neurons, by voltage clamping the cell at −60 mV and 0 mV, respectively, 2 to 3 days after tectal electroporation to express either EGFP or Rheb and EGFP in tectal neurons (Figure 6a). We first observed that in neurons co-expressing Rheb and EGFP, both amplitude (10.33 ± 0.78 pA, $n = 10$ for untransfected cells and 10.25 ± 0.93 pA, $n = 6$ for EGFP cells vs. 14.22 ± 1.14 pA, $n = 7$ for Rheb + EGFP cells) and frequency (1.09 ± 0.20 Hz, $n = 10$ for untransfected cells and 1.18 ± 0.29 Hz, $n = 6$ for EGFP cells vs. 2.92 ± 0.93 Hz, $n = 7$ for Rheb + EGFP cells) of mEPSCs were significantly increased as compared to untransfected or EGFP-only expressing neurons (Figure 6b). However, mIPSC amplitude (10.47 ± 0.85 pA, $n = 10$ for untransfected cells and 10.56 ± 1.10 pA, $n = 6$ for EGFP cells vs. 11.22 ± 0.84 pA, $n = 7$ for Rheb + EGFP cells) and frequency (0.85 ± 0.19 Hz, $n = 10$ for untransfected cells and 0.92 ± 0.19 Hz, $n = 6$ for EGFP cells vs. 1.17 ± 0.76 Hz, $n = 7$ for Rheb + EGFP cells) in these same cells were not statistically different from those measured in control neurons (Figure 6b). As a consequence, the E-I ratios for both amplitude (1.01 ± 0.06, $n = 10$ for untransfected cells and 0.99 ± 0.07, $n = 6$ for EGFP cells vs. 1.28 ± 0.07, $n = 7$ for Rheb + EGFP cells) and frequency (1.79 ± 0.37, $n = 10$ for untransfected cells and 1.38 ± 0.31, $n = 6$ for EGFP cells versus. 5.52 ± 1.26, $n = 7$ for Rheb + EGFP cells) were greatly enhanced in tectal neurons overexpressing Rheb (Figure 6c). Interestingly, neurons overexpressing Rheb were also more intrinsically excitable than untransfected or EGFP-only expressing neurons, as reflected by their increased spiking output in response to step-current injection (Supporting Figure S2).

To verify that the changes in mEPSC frequency did not result from presynaptic changes, we measured paired-pulse ratios at retinotectal synapses. We observed no difference in paired-pulse facilitation at all three inter-event intervals tested between tectal neurons from untransfected, EGFP-only or Rheb + EGFP tadpoles (Supporting Figure S3), suggesting that changes in presynaptic release probability are unlikely to account for the observed changes in mEPSC frequency.

We also assessed the effect of Rheb overexpression on synapse maturation by measuring AMPA/NMDA ratios. We observed that neurons expressing Rheb and EGFP had significantly greater synaptic AMPA/NMDA ratios than untransfected and EGFP-only expressing neurons (Figure 6d,e, 1.17 ± 0.18, $n = 12$ for untransfected + EGFP cells vs. 1.61 ± 0.19, $n = 8$ for Rheb + EGFP cells). This suggests that TORC1 activation is sufficient to increase synapse maturation and drive AMPA receptor addition at developing retinotectal synapses.

Together, these results demonstrate that TORC1 activation via Rheb overexpression selectively upregulates excitatory function without interfering with inhibitory transmission, leading to a significant imbalance of the E-I ratio in tectal neurons.

3.5 | TORC1 activation leads to a mismatch of excitatory and inhibitory visual input fields

The visual input receptive field of a tectal neuron represents the parts of the visual field where sensory stimuli can evoke synaptic responses in that neuron; it is the subthreshold receptive field. Visual input receptive fields have been shown to refine progressively in development, and during this process, excitatory and inhibitory input receptive fields adjust to match one another's retinal topography (Tao & Poo, 2005). Although altering GABA receptor activity has been reported to shape receptive field properties (Shen et al., 2011; Tao & Poo, 2005), it is unclear whether more specifically altering excitatory activity could lead to similar modifications. We, therefore, investigated the functional consequences of enhancing TORC1 activation on visually evoked responses in tectal neurons.

To map visual input receptive fields, we used a projector coupled to an optic fiber cluster to present flash stimuli at random over a 7 × 7 grid while performing whole-cell patch-clamp recordings of individual tectal neurons in immobilized tadpoles (Figure 7a). We sequentially measured excitatory and inhibitory CSCs evoked in response to the presentation of light-off stimuli in different regions of the visual field by holding the cell at −60 and 0 mV, respectively (Figure 7b).

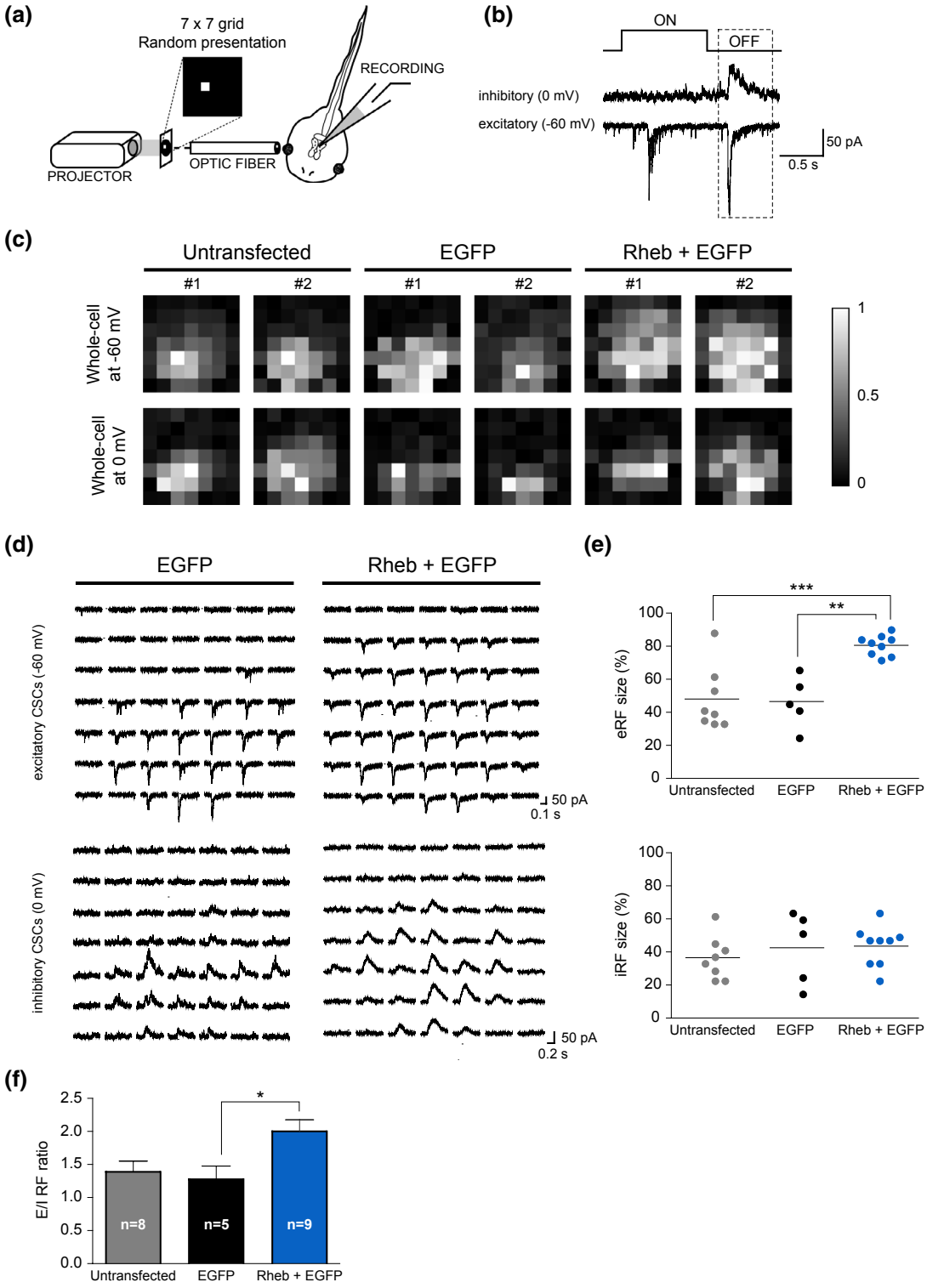

FIGURE 7 Rheb activation selectively increases excitatory visual receptive fields. (a) Schematic representation of the experimental setup. (b) Example traces of whole-cell inhibitory CSCs (recorded at 0 mV) and excitatory CSCs (recorded at −60 mV) in response to light-off stimuli. (c) Example receptive field maps for untransfected, EGFP and Rheb + EGFP expressing tectal neurons (two representative examples per condition) in gray scale, with white representing the strongest response. (d) Maps of eCSCs (−60 mV) and iCSCs (0 mV) from EGFP and Rheb + EGFP expressing cells showing light-evoked responses to stimuli in each of the 49 grid locations. (e) Graphs of excitatory and inhibitory receptive field (RF) sizes (percent of stimulation field) show that excitatory RF (top) are bigger in Rheb + EGFP expressing cells, as compared to untransfected or EGFP expressing cells (one-way ANOVA $p = .0001$ with Bonferroni post-test, $^{**}p < .01$, $^{***}p < .001$). This effect is specific to excitatory RFs, as there is no difference in inhibitory RF (bottom) size (one-way ANOVA, $p = .5848$). (f) This leads to a significant imbalance in the ratio of excitatory to inhibitory receptive field size (one-way ANOVA $p = .0282$ with Bonferroni post-test, $^{*}p < .05$) and suggests that TORC1 activation can lead to a mismatch of spatial receptive fields [Color figure can be viewed at wileyonlinelibrary.com]

For both untransfected and EGFP-expressing tectal neurons, excitatory and inhibitory receptive fields were well-matched in size and location (Figure 7c,d). This was also apparent when plotting the correlation coefficient of the strengths of excitatory versus inhibitory CSCs evoked for each individual stimulus location in the receptive field test grid (Supporting Figure S4a,b). However, for Rheb + EGFP expressing neurons, excitatory receptive fields were significantly enlarged, as compared to untransfected or EGFP-expressing neurons (Figure 7e) (47.70 ± 6.77%, $n = 8$ for untransfected cells and 46.12 ± 6.88%, $n = 5$ for EGFP cells versus. 80.50 ± 2.02%, $n = 9$ for Rheb + EGFP cells). This increase was restricted to excitatory receptive fields, as no difference was observed in the sizes of inhibitory receptive fields between the three groups (Figure 7e; 36.22 ± 4.58%, $n = 8$ for untransfected cells and 42.45 ± 9.75%, $n = 5$ for EGFP cells vs. 43.54 ± 4.07%, $n = 9$ for Rheb + EGFP cells). As a consequence, the correlation coefficient of the strength of excitatory versus. inhibitory CSCs was decreased (Supporting Figure S4, $r^2 = 0.644$, $n = 8$ for untransfected cells and $r^2 = 0.584$, $n = 5$ for EGFP cells versus. $r^2 = 0.459$, $n = 9$ for Rheb + EGFP cells) and the E-I ratio for visual receptive fields was specifically increased for Rheb + EGFP-expressing neurons (Figure 7f, 1.38 ± 0.16, $n = 8$ for untransfected cells and 1.26 ± 0.21, $n = 5$ for EGFP cells vs. 1.98 ± 0.19, $n = 9$ for Rheb + EGFP cells).

These results reveal that TORC1 activation via Rheb overexpression leads to a specific enlargement of excitatory visual input receptive fields and ultimately, to a mismatch of excitatory and inhibitory visual receptive fields, consistent with cells specifically failing to prune excitatory inputs that would normally be eliminated.

4 | DISCUSSION

In this study, we presented morphological, synaptic, and circuit level evidence that altering TORC1 signaling has a profound impact on dendritic growth and branching, as well as important effects on synaptic transmission and circuit refinement in vivo. We acutely interfered with TORC1-dependent protein synthesis by either applying rapamycin or by transfecting neurons with an antisense MO against the TORC1-specific protein Raptor and, conversely, we enhanced TORC1 activity by overexpressing Rheb, the selective upstream activator of TORC1. Activation of TORC1 by Rheb overexpression caused an increase in the number and efficacy of excitatory, but not inhibitory, synapses by favoring the delivery of AMPA receptors to nascent excitatory synapses. This, in turn, resulted in a dramatic imbalance in the E-I ratio. Furthermore, individual tectal neurons were found to have greatly expanded excitatory visual input fields, without comparable inhibitory modulation, which would be expected to seriously impact sensory processing of visual information in the optic tectum. Although other groups have taken an interest in studying the role of protein synthesis in the development and establishment of dendritic morphology and brain circuits (Bateup et al., 2011, 2013; Chow et al., 2009; Gkogkas et al., 2013; Jaworski et al., 2005; Kumar et al., 2005; Tavazoie et al., 2005), our study is one of the few to investigate the consequences of altering TORC1-dependent protein synthesis in single neurons in an intact circuit in vivo, allowing us to avoid many of the pitfalls of network-wide activity dysregulation. Interestingly, our observation that upregulation and downregulation of TORC1 activity had opposite effects on excitatory synaptic maturation and dendritic arborization, suggests that relative levels of mTOR-dependent translation may regulate the total levels of excitatory input that a neuron receives.

4.1 | Activity-dependent dendritic growth and TORC1-dependent synaptic maturation

The synaptotropic hypothesis, which was originally formulated by Vaughn, states that as neuronal processes extend toward regions where they are likely to find synaptic partners, their growth and branching are most likely to occur in those regions of the arbor where they have established a stable synapse (Vaughn, 1989). Moreover, previous work has demonstrated that interfering with the trafficking of AMPA receptors to nascent synapses can dramatically impair dendritic arborization (Haas et al., 2006). In other words, failure to incorporate AMPA receptors at NMDAR-only containing synapses prevents the synaptic maturation of developing synapses, as well as the stabilization of dendritic arbors. These studies, therefore, support the idea that dendritic arbor stabilization and synaptic maturation are mechanistically related events (Cline & Haas, 2008; Wu et al., 1999).

In line with those experiments, our work now reports that the TORC1-dependent addition of new AMPA receptors at developing synapses correlated with significantly bigger and more branched dendritic arbors, which lends additional support to the synaptotropic hypothesis. Activation of TORC1-dependent protein synthesis might upregulate the levels of proteins that are required to stabilize nascent synapses, and, therefore, "prime" or "tag" those same synapses for long-term changes, which would in turn support further growth of the dendritic arbor. This is reminiscent of the phenomena of synaptic tagging and late-phase long-term potentiation. During plasticity paradigms in the adult brain, synapses that have been tagged by previous synaptic activity are able to capture plasticity-related proteins and convert short-term synaptic modifications into long-term synaptic changes (Frey & Morris, 1997). Moreover, recent evidence has raised the intriguing possibility that ongoing TORC1-dependent

protein translation might itself act as a synaptic tag per se (Sosanya et al., 2015).

4.2 | TORC1-dependent protein synthesis of molecular components of excitatory synapses

Our study reports that activation of TORC1 favors the maturation of retinotectal synapses, as reflected by the addition of new AMPA receptors to synapses. Although our results point to a TORC1-dependent upregulation of AMPA receptors, it is unlikely that de novo synthesis of AMPA receptors is a limiting factor for the initial stages of retinotectal synapse maturation. Indeed, it has been shown that the conversion of NMDAR-containing silent synapses into functional synapses at normal resting potentials can occur within minutes (Liao et al., 2001), probably through lateral diffusion and activity-dependent synaptic trapping of existing AMPA receptors (Groc et al., 2006; Opazo & Choquet, 2011). However, local dendritic translation could well exert an influence on the relative stoichiometry of subunits that are available to compose local AMPA receptors. It is interesting to note that exposure to the pro-inflammatory cytokine Tumor Necrosis Factor α, which mediates the phenomenon of homeostatic synaptic scaling in which GluA2-lacking receptors are disproportionately delivered to synapses, appears to have very similar effects to those we report for TORC1 activation on neuronal morphogenesis and circuit function, consistent with synaptic AMPA receptor subunit composition impacting long-term changes in dendritic growth and wiring specificity (Lee et al., 2010; Soares et al., 2013; Stellwagen & Malenka, 2006). Previous work has shown that the trafficking of new AMPA receptors is necessary to stabilize nascent synapses and promote dendritic branch elaboration, and that different cell types may be differentially affected by specific AMPA subunits (Haas et al., 2006; He et al., 2018). Enhancement of the TORC1 pathway via 4E-BP2 knock-out in hippocampal neurons has previously been shown to upregulate the synthesis of GluA1 and GluA2 subunits (Ran et al., 2013). We now demonstrate in developing Xenopus tadpoles that both GluA1 and GluA2 expression levels are reduced when TORC1 is inhibited by rapamycin treatment.

There is also evidence to suggest that GluN2B-containing NMDA receptors which are predominant during early development, prevent the activation of mTOR-dependent translation, the synthesis of the AMPA receptor subunits GluA1 and GluA2, as well as the synaptic incorporation of AMPA receptors at nascent synapses (Ferreira et al., 2015; Hall et al., 2007; Sutton et al., 2006; Wang et al., 2011). The developmental switch from GluN2B- to GluN2A-containing NMDA receptors would then alleviate the brake on protein synthesis and favor the addition of AMPA receptors to activated synapses (Gray et al., 2011; Kim et al., 2005; Wang et al., 2011). It is, therefore, tempting to speculate that in our model, activation of TORC1 by Rheb overexpression could bypass the constraint imposed by NMDA receptors and constitutively turn on the synthesis of synaptic proteins that are necessary to drive the maturation of synapses. Although activity-dependent translation of AMPA receptors has been reported (Ju et al., 2004) and might be important to sustain synaptic changes at developing synapses, the activity-dependent incorporation or synthesis of other postsynaptic density scaffolding proteins such as neuroligins (Chubykin et al., 2007; Letellier et al., 2018), PSD-MAGUKS (Elias et al., 2006), Shank3 (Roussignol et al., 2005) or auxiliary proteins such as SynDIG1 (Chenaux et al., 2016; Kalashnikova et al., 2010; Lovero et al., 2013), SynDIG4 (Matt et al., 2018), and TARPs (Hall et al., 2007; Rouach et al., 2005) might also be critical for synaptic maturation.

4.3 | TORC1-dependent regulation of the excitation-to-inhibition balance

Our experiments have demonstrated that activation of the mTOR pathway has a very specific effect on excitatory synapses with no apparent effects on inhibitory synapses, as we could not detect any changes in the amplitude or frequency of GABA-mediated mIPSCs. This, therefore, suggests that TORC1 activation may have resulted in a selective upregulation of proteins that are required to assemble excitatory synapses and cluster AMPA receptors to developing synapses (Favuzzi & Rico, 2018; Thoreen et al., 2012).

Among the candidate proteins listed above, neuroligins are of particular interest. Indeed, neuroligin-1 is specifically enriched at excitatory synapses while neuroligin-2 is enriched at inhibitory synapses (Chih et al., 2005; Chubykin et al., 2007; Graf et al., 2004) and it has been suggested that their relative expression could control the E-I balance (Levinson & El-Husseini, 2005). Moreover, previous studies have reported that dysregulation of the mTOR pathway could alter the protein levels of neuroligins (Gkogkas et al., 2013). Alternatively, increased levels of PSD-95 might favor the assembly of excitatory synapses by clustering neuroligin-1 and PSD-95 at excitatory synapses (Prange et al., 2004) or trigger the redistribution of neuroligin-2 from inhibitory to excitatory synapses (Levinson et al., 2005).

It is noteworthy that other studies have described that interfering with the mTOR pathway had diverse effects on inhibitory transmission (Bateup et al., 2013; Gkogkas et al., 2013). Although the alterations of synaptic transmission reported by Gkokas and co-workers were mostly attributed to changes in excitatory transmission, in

keeping with our results, Bateup and colleagues reported that knockdown of Tsc1 did not affect excitatory transmission, which is in stark contrast with our findings. In fact, they reported that knockdown of Tsc1 in postsynaptic neurons dramatically reduced presynaptic inhibitory function, which suggests another potential role for TORC1 in regulating homeostatic feedback to presynaptic inhibitory inputs and that the loss of inhibition was secondary to the dysregulation of mTOR. It is also important to note that, as opposed to previous studies, our work utilized a very sparse and temporally restricted knockdown or activation of TORC1 in an in vivo model. Global activation of mTOR for prolonged periods of time might lead to compensatory changes in a network that is already in a hyperactivated and unstable state, thereby yielding different outcomes from what we report here. Previous work has indeed described how TORC1 activity in postsynaptic neurons can drive homeostatic changes in neurotransmitter release from the presynaptic side (Henry et al., 2012). Alternatively, it has also been reported that global knockdown of synaptic proteins might have very different effects than sparse knockdown, as illustrated by work on neuroligin-1. Effects on synapse formation and synaptic maturation were only observed when neuroligin-1 was differentially expressed in neurons, underlining the importance of competitive processes during synaptogenesis (Kwon et al., 2012).

Finally, although our results have clearly highlighted a role for TORC1-dependent translation in the stabilization and maturation of developing retinotectal synapses, it remains to be determined whether the initiation of new protein synthesis takes place in the cell body or whether it is more spatially restricted to dendritic branches or activated synapses. Many studies have indeed underlined the role of TORC1-dependent local protein synthesis to support synaptic changes in the adult brain (Aakalu et al., 2001; Cracco et al., 2005; Takei et al., 2004) and it would be interesting to see if the same rules govern the stabilization of nascent synapses during early development in vivo. Alternatively, compelling experimental evidence suggests that initiation of translation may merely be permissive (and, therefore, rate-limiting) for protein synthesis-dependent plasticity, with local translation and targeting of new proteins governed by the elongation of nascent proteins at stalled polysomes transported to relevant sites of synaptic plasticity (Graber et al., 2013).

It is also possible to conceive of a scenario in which nonspecific cellular changes could engage synaptic plasticity mechanisms to produce the changes we observed. For example, a cell-wide upregulation of voltage-gated ion channels, enhancing intrinsic excitability, could extend Hebbian mechanisms, which normally promote the maturation of synapses formed by convergent cooperative inputs, to a larger number of more diffuse inputs, now rendered capable of driving action potential firing in the postsynaptic neuron (Aizenman et al., 2003; Munz et al., 2014; Spratt et al., 2019). Indeed, we observed that Rheb overexpression did lead to enhanced intrinsic excitability of tectal neurons.

Single-gene mutations of key components of the mTOR/PI3K pathway such as Tsc1/Tsc2 and PTEN, associated translational repressors such as FMRP, as well as neuroligins are thought to underlie several neurodevelopmental disorders associated with autism including tuberous sclerosis (Bateup et al., 2011, 2013; Kwiatkowski & Manning, 2005) and Fragile X syndrome (Bagni & Greenough, 2005; Sharma et al., 2010). In fact, one of the predominant hypotheses is that the disruption of components of the mTOR/PI3K pathway leads to dysregulation of protein synthesis that in turn alters the number and the strength of excitatory connections and ultimately the balance of excitation-to-inhibition in specific circuits (Bourgeron, 2009; Kelleher & Bear, 2008). Furthering our understanding of the cellular and molecular mechanisms that participate in the proper wiring of the brain and the refinement of specific synaptic connections can hopefully shed light on the mechanistic underpinnings of complex neurological disorders that result from neuronal wiring abnormalities during early brain development, such as ASDs, schizophrenia, and epilepsy.

ACKNOWLEDGMENTS

The authors thank all the members of the Ruthazer lab for comments and insightful discussions on the project and the manuscript. The authors also thank Dr. C. Aizenman (Brown University), Dr. K. Pratt (University of Wyoming), and Dr. A. Khakhalin (Bard College) for excellent advice on electrophysiology experiments, Dr. W. Sossin for invaluable advice and discussions, as well as Dr. K. Haas (University of British Columbia) for advice on single-cell electroporation. This work was supported by a Fonds de la Recherche du Québec—Santé postdoctoral fellowship to D.G. and research grant from the Canadian Institutes for Health Research (FDN-143238) to E.S.R.

CONFLICT OF INTERESTS

The authors declare that there are no conflicts of interest.

AUTHOR CONTRIBUTIONS

Conceptualization: Gobert and Ruthazer
Methodology: Gobert and Schohl
Formal Analysis: Gobert
Investigation: Gobert, Schohl, and Kutsarova
Writing—Original Draft: Gobert
Writing—Review & Editing: Schohl, Kutsarova and Ruthazer
Visualization: Gobert and Ruthazer
Supervision: Ruthazer
Funding Acquisition: Ruthazer

DATA AVAILABILITY STATEMENT

All raw data and molecular constructs will be freely shared upon request.

ORCID

Edward S. Ruthazer https://orcid.org/0000-0003-0452-3151

REFERENCES

Aakalu, G., Smith, W. B., Nguyen, N., Jiang, C., & Schuman, E. M. (2001). Dynamic visualization of local protein synthesis in hippocampal neurons. *Neuron*, *30*(2), 489–502.

Aizenman, C. D., Akerman, C. J., Jensen, K. R., & Cline, H. T. (2003). Visually driven regulation of intrinsic neuronal excitability improves stimulus detection in vivo. *Neuron*, *39*(5), 831–842.

Antoine, M. W., Langberg, T., Schnepel, P., & Feldman, D. E. (2019). Increased excitation-inhibition ratio stabilizes synapse and circuit excitability in four autism mouse models. *Neuron*, *101*, 648–661.

Bagni, C., & Greenough, W. T. (2005). From mRNP trafficking to spine dysmorphogenesis: The roots of fragile X syndrome. *Nature Reviews Neuroscience*, *6*(5), 376–387.

Bateup, H. S., Johnson, C. A., Denefrio, C. L., Saulnier, J. L., Kornacker, K., & Sabatini, B. L. (2013). Excitatory/inhibitory synaptic imbalance leads to hippocampal hyperexcitability in mouse models of tuberous sclerosis. *Neuron*, *78*(3), 510–522.

Bateup, H. S., Takasaki, K. T., Saulnier, J. L., Denefrio, C. L., & Sabatini, B. L. (2011). Loss of Tsc1 in vivo impairs hippocampal mGluR-LTD and increases excitatory synaptic function. *Journal of Neuroscience*, *31*(24), 8862–8869.

Bourgeron, T. (2009). A synaptic trek to autism. *Current Opinion in Neurobiology*, *19*(2), 231–234. Review.

Chenaux, G., Matt, L., Hill, T. C., Kaur, I., Liu, X. B., Kirk, L. M., Speca, D. J., McMahon, S. A., Zito, K., Hell, J. W., & Díaz, E. (2016). Loss of SynDIG1 reduces excitatory synapse maturation but not formation in vivo. *eNeuro*, *3*(5), pii: ENEURO.0130-16.

Chih, B., Engelman, H., & Scheiffele, P. (2005). Control of excitatory and inhibitory synapse formation by neuroligins. *Science*, *307*(5713), 1324–1328.

Chow, D. K., Groszer, M., Pribadi, M., Machniki, M., Carmichael, S. T., Liu, X., & Trachtenberg, J. T. (2009). Laminar and compartmental regulation of dendritic growth in mature cortex. *Nature Neuroscience*, *12*(2), 116–118.

Chubykin, A. A., Atasoy, D., Etherton, M. R., Brose, N., Kavalali, E. T., Gibson, J. R., & Südhof, T. C. (2007). Activity-dependent validation of excitatory versus inhibitory synapses by neuroligin-1 versus neuroligin-2. *Neuron*, *54*(6), 919–931.

Cline, H., & Haas, K. (2008). The regulation of dendritic arbor development and plasticity by glutamatergic synaptic input: A review of the synaptotrophic hypothesis. *The Journal of Physiology*, *586*(6), 1509–1517. Review.

Coupé, P., Munz, M., Manjón, J. V., Ruthazer, E. S., & Collins, D. L. (2012). A CANDLE for a deeper in vivo insight. *Medical Image Analysis*, *16*(4), 849–864.

Cracco, J. B., Serrano, P., Moskowitz, S. I., Bergold, P. J., & Sacktor, T. C. (2005). Protein synthesis-dependent LTP in isolated dendrites of CA1 pyramidal cells. *Hippocampus.*, *15*(5), 551–556.

Elias, G. M., Funke, L., Stein, V., Grant, S. G., Bredt, D. S., & Nicoll, R. A. (2006). Synapse-specific and developmentally regulated targeting of AMPA receptors by a family of MAGUK scaffolding proteins. *Neuron*, *52*(2), 307–320.

Favuzzi, E.,&Rico B. (2018). Molecular diversity underlying cortical excitatory and inhibitory synapse development. *Current Opinion in Neurobiology*, *53*, 8–15. Review.

Ferreira, J. S., Schmidt, J., Rio, P., Águas, R., Rooyakkers, A., Li, K. W., Smit, A. B., Craig, A. M., & Carvalho, A. L. (2015). GluN2B-containing NMDA receptors regulate AMPA receptor traffic through anchoring of the synaptic proteasome. *Journal of Neuroscience*, *35*(22), 8462–8479.

Frey, U., & Morris, R. G. (1997). Synaptic tagging and long-term potentiation. *Nature*, *385*(6616), 533–536.

Gkogkas, C. G., Khoutorsky, A., Ran, I., Rampakakis, E., Nevarko, T., Weatherill, D. B., Vasuta, C., Yee, S., Truitt, M., Dallaire, P., Major, F., Lasko, P., Ruggero, D., Nader, K., Lacaille, J. C., & Sonenberg, N. (2013). Autism-related deficits via dysregulated eIF4E-dependent translational control. *Nature*, *493*(7432), 371–377.

Graber, T. E., Hébert-Seropian, S., Khoutorsky, A., David, A., Yewdell, J. W., Lacaille, J. C., & Sossin, W. S. (2013). Reactivation of stalled polyribosomes in synaptic plasticity. *Proceedings of the National Academy of Sciences USA*, *110*(40), 16205–16210.

Graf, E. R., Zhang, X., Jin, S. X., Linhoff, M. W., & Craig, A. M. (2004). Neurexins induce differentiation of GABA and glutamate postsynaptic specializations via neuroligins. *Cell*, *119*(7), 1013–1026.

Gray, J. A., Shi, Y., Usui, H., During, M. J., Sakimura, K., & Nicoll, R. A. (2011). Distinct modes of AMPA receptor suppression at developing synapses by GluN2A and GluN2B: Single-cell NMDA receptor subunit deletion in vivo. *Neuron*, *71*(6), 1085–1101.

Groc L., Gustafsson B., & Hanse, E. (2006). AMPA signalling in nascent glutamatergic synapses: There and not there! *Trends in Neurosciences*, *29*(3), 132–139. Review.

Haas, K., Li, J., & Cline, H. T. (2006). AMPA receptors regulate experience-dependent dendritic arbor growth in vivo. *Proceedings of the National Academy of Sciences of the USA*, *103*(32), 12127–12131.

Hall, B. J., Ripley, B., & Ghosh, A. (2007). NR2B signaling regulates the development of synaptic AMPA receptor current. *Journal of Neuroscience*, *27*(49), 13446–13456.

Hay, N., & Sonenberg, N. (2004). Upstream and downstream of mTOR. *Genes & Development*, *18*(16), 1926–1945.

He, H. Y., Shen, W., Zheng, L., Guo, X., & Cline, H. T. (2018). Excitatory synaptic dysfunction cell-autonomously decreases inhibitory inputs and disrupts structural and functional plasticity. *Nature Communications*, *9*(1), 2893.

Henry, F. E., Hockeimer, W., Chen, A., Mysore, S. P., & Sutton, M. A. (2017). Mechanistic target of rapamycin is necessary for changes in dendritic spine morphology associated with long-term potentiation. *Molecular Brain*, *10*(1), 50.

Henry, F. E., McCartney, A. J., Neely, R., Perez, A. S., Carruthers, C. J., Stuenkel, E. L., Inoki, K., & Sutton, M. A. (2012). Retrograde changes in presynaptic function driven by dendritic mTORC1. *Journal of Neuroscience*, *32*(48), 17128–17142.

Huang, J., & Manning, B. D. (2008). The TSC1-TSC2 complex: A molecular switchboard controlling cell growth. *Biochemical Journal*, *412*(2), 179–190. Review.

Jaworski, J., Spangler, S., Seeburg, D. P., Hoogenraad, C. C., & Sheng, M. (2005). Control of dendritic arborization by the phosphoinositide-3'-kinase-Akt-mammalian target of rapamycin pathway. *Journal of Neuroscience*, *25*(49), 11300–11312.

Ju, W., Morishita, W., Tsui, J., Gaietta, G., Deerinck, T. J., Adams, S. R., Garner, C. C., Tsien, R. Y., Ellisman, M. H., & Malenka, R. C. (2004). Activity-dependent regulation of dendritic synthesis and trafficking of AMPA receptors. *Nature Neuroscience*, *7*(3), 244–253.

Kalashnikova, E., Lorca, R. A., Kaur, I., Barisone, G. A., Li, B., Ishimaru, T., Trimmer, J. S., Mohapatra, D. P., & Díaz, E. (2010). SynDIG1: An activity-regulated, AMPA- receptor-interacting transmembrane protein that regulates excitatory synapse development. *Neuron*, *65*(1), 80–93.

Kelleher, R. J. 3rd, & Bear, M. F. (2008). The autistic neuron: Troubled translation? *Cell*, *135*(3), 401–406.

Kim, M. J., Dunah, A. W., Wang, Y. T., & Sheng, M. (2005). Differential roles of NR2A- and NR2B-containing NMDA receptors in Ras-ERK signaling and AMPA receptor trafficking. *Neuron*, *46*(5), 745–760.

Kumar, V., Zhang, M. X., Swank, M. W., Kunz, J., & Wu, G. Y. (2005). Regulation of dendritic morphogenesis by Ras-PI3K-Akt-mTOR and Ras-MAPK signaling pathways. *Journal of Neuroscience*, *25*(49), 11288–11299.

Kwiatkowski, D. J., & Manning, B. D. (2005). Tuberous sclerosis: A GAP at the crossroads of multiple signaling pathways. *Human Molecular Genetics*, 14 Spec No. 2:R251–R258. Review.

Kwon, H. B., Kozorovitskiy, Y., Oh, W. J., Peixoto, R. T., Akhtar, N., Saulnier, J. L., Gu, C., & Sabatini, B. L. (2012). Neuroligin-1-dependent competition regulates cortical synaptogenesis and synapse number. *Nature Neuroscience*, *15*(12), 1667–1674.

Lee, R. H., Mills, E. A., Schwartz, N., Bell, M. R., Deeg, K. E., Ruthazer, E. S., Marsh-Armstrong, N., & Aizenman, C. D. (2010). Neurodevelopmental effects of chronic exposure to elevated levels of pro-inflammatory cytokines in a developing visual system. *Neural Development*, *5*, 2.

Letellier, M., Szíber, Z., Chamma, I., Saphy, C., Papasideri, I., Tessier, B., Sainlos, M., Czöndör, K., & Thoumine, O. (2018). A unique intracellular tyrosine in neuroligin-1 regulates AMPA receptor recruitment during synapse differentiation and potentiation. *Nature Communications*, *9*(1), 3979.

Levinson, J. N., Chéry, N., Huang, K., Wong, T. P., Gerrow, K., Kang, R., Prange, O., Wang, Y. T., & El-Husseini, A. (2005). Neuroligins mediate excitatory and inhibitory synapse formation: Involvement of PSD-95 and neurexin-1beta in neuroligin-induced synaptic specificity. *Journal of Biological Chemistry*, *280*(17), 17312–17319.

Levinson, J. N., & El-Husseini, A. (2005). Building excitatory and inhibitory synapses: Balancing neuroligin partnerships. *Neuron*, *48*(2), 171–174.

Liao, D., Hessler, N. A., & Malinow, R. (1995). Activation of postsynaptically silent synapses during pairing-induced LTP in CA1 region of hippocampal slice. *Nature*, *375*(6530), 400–404.

Liao, D., Scannevin, R. H., & Huganir, R. (2001). Activation of silent synapses by rapid activity-dependent synaptic recruitment of AMPA receptors. *Journal of Neuroscience*, *21*(16), 6008–6017.

Lovero, K. L., Blankenship, S. M., Shi, Y., & Nicoll, R. A. (2013). SynDIG1 promotes excitatory synaptogenesis independent of AMPA receptor trafficking and biophysical regulation. *PLoS ONE*, *8*(6), e66171.

Matt, L., Kirk, L. M., Chenaux, G., Speca, D. J., Puhger, K. R., Pride, M. C., Qneibi, M., Haham, T., Plambeck, K. E., Stern-Bach, Y., Silverman, J. L., Crawley, J. N., Hell, J. W., & Díaz, E. (2018). SynDIG4/Prrt1 is required for excitatory synapse development and plasticity underlying cognitive function. *Cell Reports*, *22*(9), 2246–2253.

Munz, M., Gobert, D., Schohl, A., Poquérusse, J., Podgorski, K., Spratt, P., & Ruthazer, E. S. (2014). Rapid Hebbian axonal remodeling mediated by visual stimulation. *Science*, *344*(6186), 904–909.

Opazo, P., & Choquet, D. (2011). A three-step model for the synaptic recruitment of AMPA receptors. *Molecular and Cellular Neurosciences*, *46*(1), 1–8.

Prange, O., Wong, T. P., Gerrow, K., Wang, Y. T., & El-Husseini, A. (2004). A balance between excitatory and inhibitory synapses is controlled by PSD-95 and neuroligin. *Proceedings of the National Academy of Sciences of the USA*, *101*(38), 13915–13920.

Rajan, I., & Cline, H. T. (1998). Glutamate receptor activity is required for normal development of tectal cell dendrites in vivo. *Journal of Neuroscience*, *18*(19), 7836–7846.

Ran, I., Gkogkas, C. G., Vasuta, C., Tartas, M., Khoutorsky, A., Laplante, I., Parsyan, A., Nevarko, T., Sonenberg, N., & Lacaille, J. C. (2013). Selective regulation of GluA subunit synthesis and AMPA receptor-mediated synaptic function and plasticity by the translation repressor 4E-BP2 in hippocampal pyramidal cells. *Journal of Neuroscience*, *33*(5), 1872–1886.

Rouach, N., Byrd, K., Petralia, R. S., Elias, G. M., Adesnik, H., Tomita, S., Karimzadegan, S., Kealey, C., Bredt, D. S., & Nicoll, R. A. (2005). TARP gamma-8 controls hippocampal AMPA receptor number, distribution and synaptic plasticity. *Nature Neuroscience*, *8*(11), 1525–1533.

Roussignol, G., Ango, F., Romorini, S., Tu, J. C., Sala, C., Worley, P. F., Bockaert, J., & Fagni, L. (2005). Shank expression is sufficient to induce functional dendritic spine synapses in aspiny neurons. *Journal of Neuroscience*, *25*(14), 3560–3570.

Ruthazer, E. S., Haas, K., Javaherian, A., Jensen, K. R., Sin, W. C., & Cline, H. (2005). In vivo time-lapse imaging of neuronal development. In R. Yuste & A. Konnerth (Eds.), *Imaging in neuroscience and development: A laboratory manual* (pp. 191–204). Cold Spring Harbor Laboratory Press.

Sarbassov, D. D., Ali, S. M., Sengupta, S., Sheen, J. H., Hsu, P. P., Bagley, A. F., Markhard, A. L., & Sabatini, D. M. (2006). Prolonged rapamycin treatment inhibits mTORC2 assembly and Akt/PKB. *Molecular Cell*, *22*(2), 159–168.

Saxton R. A., & Sabatini D. M. (2017). mTOR signaling in growth, metabolism, and disease. *Cell*, *168*(6), 960–976. Review.

Sharma, A., Hoeffer, C. A., Takayasu, Y., Miyawaki, T., McBride, S. M., Klann, E., & Zukin, R. S. (2010). Dysregulation of mTOR signaling in fragile X syndrome. *Journal of Neuroscience*, *30*(2), 694–702.

Shen, W., McKeown, C. R., Demas, J. A., & Cline, H. T. (2011). Inhibition to excitation ratio regulates visual system responses and behavior in vivo. *Journal of Neurophysiology*, *106*(5), 2285–2302.

Skalecka, A., Liszewska, E., Bilinski, R., Gkogkas, C., Khoutorsky, A., Malik, A. R., Sonenberg, N., & Jaworski, J. (2016). mTOR kinase is needed for the development and stabilization of dendritic arbors in newly born olfactory bulb neurons. *Developmental Neurobiology*, *76*(12), 1308–1327.

Soares, C., Lee, K. F. H., Nasrallah, W., & Béïque, J. C. (2013). Differential subcellular targeting of glutamate receptor subtypes during homeostatic synaptic plasticity. *Journal of Neuroscience*, *33*(33), 13547–13559.

Sosanya, N. M., Cacheaux, L. P., Workman, E. R., Niere, F., Perrone-Bizzozero, N. I., & Raab-Graham, K. F. (2015). Mammalian target of rapamycin (mTOR) tagging promotes dendritic branch variability

through the capture of Ca2+/calmodulin-dependent protein kinase II α (CaMKIIα) mRNAs by the RNA-binding protein HuD. *Journal of Biological Chemistry*, *290*(26), 16357–16371.

Spratt, P. W. E., Ben-Shalom, R., Keeshen, C. M., Burke, K. J. Jr, Clarkson, R. L., Sanders, S. J., & Bender, K. J. (2019). The autism-associated gene Scn2a contributes to dendritic excitability and synaptic function in the prefrontal cortex. *Neuron*, *103*(4), 673–685.

Stellwagen, D., & Malenka, R. C. (2006). Synaptic scaling mediated by glial TNF-alpha. *Nature*, *440*(7087), 1054–1059.

Sutton, M. A., Ito, H. T., Cressy, P., Kempf, C., Woo, J. C., & Schuman, E. M. (2006). Miniature neurotransmission stabilizes synaptic function via tonic suppression of local dendritic protein synthesis. *Cell*, *125*(4), 785–799.

Switon, K., Kotulska, K., Janusz-Kaminska, A., Zmorzynska, J., & Jaworski, J. (2017). Molecular neurobiology of mTOR. *Neuroscience*, *341*, 112–153.

Takei, N., Inamura, N., Kawamura, M., Namba, H., Hara, K., Yonezawa, K., & Nawa, H. (2004). Brain-derived neurotrophic factor induces mammalian target of rapamycin-dependent local activation of translation machinery and protein synthesis in neuronal dendrites. *Journal of Neuroscience*, *24*(44), 9760–9769.

Tao, H. W., & Poo, M. M. (2005). Activity-dependent matching of excitatory and inhibitory inputs during refinement of visual receptive fields. *Neuron*, *45*(6), 829–836.

Tavazoie, S. F., Alvarez, V. A., Ridenour, D. A., Kwiatkowski, D. J., & Sabatini, B. L. (2005). Regulation of neuronal morphology and function by the tumor suppressors Tsc1 and Tsc2. *Nature Neuroscience*, *8*(12), 1727–1734.

Thoreen, C. C., Chantranupong, L., Keys, H. R., Wang, T., Gray, N. S., & Sabatini, D. M. (2012). A unifying model for mTORC1-mediated regulation of mRNA translation. *Nature*, *485*(7396), 109–113.

Vaughn, J. E. (1989). Fine structure of synaptogenesis in the vertebrate central nervous system. *Synapse*, *3*(3), 255–285. Review.

Wang, C. C., Held, R. G., Chang, S. C., Yang, L., Delpire, E., Ghosh, A., & Hall, B. J. (2011). A critical role for GluN2B-containing NMDA receptors in cortical development and function. *Neuron*, *72*(5), 789–805.

Wu, G., Malinow, R., & Cline, H. T. (1996). Maturation of a central glutamatergic synapse. *Science*, *274*(5289), 972–976.

Wu, G. Y., Zou, D. J., Rajan, I., & Cline, H. (1999). Dendritic dynamics in vivo change during neuronal maturation. *Journal of Neuroscience*, *19*(11), 4472–4483.

SUPPORTING INFORMATION

Additional supporting information may be found online in the Supporting Information section.

How to cite this article: Gobert D, Schohl A, Kutsarova E, Ruthazer ES. TORC1 selectively regulates synaptic maturation and input convergence in the developing visual system. *Develop Neurobiol*. 2020;80:332–350. https://doi.org/10.1002/dneu.22782